VIBRATION ANALYSIS OF CANTILEVERED CURVED PLATES
USING A NEW CYLINDRICAL SHELL FINITE ELEMENT

Mervyn D. Olson* and Garry M. Lindberg**

National Aeronautical Establishment,

Ottawa, Canada

The stiffness and mass matrices for a relatively simple finite cylindrical shell element are presented. The element has 28 degrees of freedom corresponding to the seven generalized coordinates $\partial w/\partial x$, $\partial w/\partial y$, w, $\partial u/\partial y$, u, $\partial v/\partial y$, and v at each corner. All six rigid body modes for the element are adequately represented by this model. The element is used to predict the vibrations of a curved fan blade, and the results are verified experimentally. It is found that a 4 x 4 grid of the finite elements is sufficient to predict the first twelve vibration frequencies for the fan blade to within ten percent. The agreement between experimental and theoretical mode shapes is generally very good.

---

* Assistant Research Officer, Structures and Materials Laboratory

** Associate Research Officer, Structures and Materials Laboratory

Report Documentation Page

Public reporting burden for the collection of information is estimated to average 1 hour per response, including the time for reviewing instructions, searching existing data sources, gathering and maintaining the data needed, and completing and reviewing the collection of information. Send comments regarding this burden estimate or any other aspect of this collection of information, including suggestions for reducing this burden, to Washington Headquarters Services, Directorate for Information Operations and Reports, 1215 Jefferson Davis Highway, Suite 1204, Arlington VA 22202-4302. Respondents should be aware that notwithstanding any other provision of law, no person shall be subject to a penalty for failing to comply with a collection of information if it does not display a currently valid OMB control number.

1. REPORT DATE **OCT 1968**	2. REPORT TYPE	3. DATES COVERED **00-00-1968 to 00-00-1968**

4. TITLE AND SUBTITLE **Vibration Analysis of Cantilevered Curved Plates Using a New Cylindrical Shell Finite Element**	5a. CONTRACT NUMBER
	5b. GRANT NUMBER
	5c. PROGRAM ELEMENT NUMBER
6. AUTHOR(S)	5d. PROJECT NUMBER
	5e. TASK NUMBER
	5f. WORK UNIT NUMBER

7. PERFORMING ORGANIZATION NAME(S) AND ADDRESS(ES) **Air Force Flight Dynamics Laboratory,Wright Patterson AFB,OH,45433**	8. PERFORMING ORGANIZATION REPORT NUMBER
9. SPONSORING/MONITORING AGENCY NAME(S) AND ADDRESS(ES)	10. SPONSOR/MONITOR'S ACRONYM(S)
	11. SPONSOR/MONITOR'S REPORT NUMBER(S)

12. DISTRIBUTION/AVAILABILITY STATEMENT **Approved for public release; distribution unlimited**

13. SUPPLEMENTARY NOTES **See also AD0703685, Proceedings of the Conference on Matrix Methods in Structural Mechanics (2nd) Held at Wright-Patterson Air Force Base, Ohio, on 15-17 October 1968.**

14. ABSTRACT

15. SUBJECT TERMS

16. SECURITY CLASSIFICATION OF:			17. LIMITATION OF ABSTRACT	18. NUMBER OF PAGES **24**	19a. NAME OF RESPONSIBLE PERSON
a. REPORT **unclassified**	b. ABSTRACT **unclassified**	c. THIS PAGE **unclassified**			

SECTION I

INTRODUCTION

Considerable progress has been made in the past few years in applying the finite element method to the analysis of shell structures. The majority of the work has been devoted to shells of revolution in which closed rings or conical shell segments are used in the modelling of complete structures. Most of this work is reviewed in Reference 1.

Attempts to develop a finite element method for general shell structures have taken two different approaches. In the first approach, the shell is replaced by an assemblage of flat plate elements which are either triangular or quadrilateral in shape. Each plate element is connected in some fashion to those surrounding it and undergoes both bending and stretching deformations. This approach has been successfully used for cylindrical geometry in Reference 2 and for general shell shapes in Reference 3. The second approach, which ultimately should give better results, is to develop curved shell elements that permit exact geometrical representations of a structure. Initial attempts to derive such a curved finite element for an arbitrary shell have been only partially successful (Reference 4). Since such a development would be a major accomplishment, it appears feasible to approach the problem more slowly by setting up models for particular shell configurations, such as cylindrical, conical, spherical, and so on. The logical one to begin with is of course the cylindrical shell partly because it is geometrically the simplest and also because the practical applications are so numerous. The first start in this direction was made by Bogner, Fox and Schmit (Reference 5).

The element presented in Reference 5 has 48 degrees of freedom and the authors state that an assemblage of their elements is geometrically admissible (i.e., has continuous zero and first derivatives of the displacements along element interfaces) and therefore guarantees monotonic convergence of the total potential energy as the modelling is successively refined. The example application presented in Reference 5, the pinched cylinder problem discussed by Timoshenko in Reference 6, is essentially a ring-bending problem and is therefore not an adequate test of their shell element. Furthermore, 48 degrees of freedom per element seem to be more than necessary to ensure geometrical admissibility. That is, according to the convergence proof in Reference 7, piecewise continuity of the first derivatives of the in-plane displacements and of the second derivatives of the out-of-plane displacement are sufficient conditions for monotonic convergence of the total potential energy. Hence, it appears that this 48 degrees of freedom model is not the most efficient representation because extra degrees of freedom are included to ensure piecewise continuity of the second derivatives of the in-plane displacements.

Since the work reported herein was completed, another cylindrical shell finite element representation with only 24 degrees of freedom has been published by Cantin and Clough (Reference 8). The displacement functions assumed for this element include terms which couple the u, v and w displacements in such a way that all six rigid body modes for the element are represented exactly. Further, when the shell radius goes to infinity, these displacements reduce to the conforming flat plate case. However, it is not clear whether or not their element is conforming for arbitrary shell radii. The example applications given in Reference 8 indicate that this element works well for static problems but no dynamic solutions have been presented.

There is still some question as to the necessity of completely conforming (continuous normal derivatives at element interfaces) finite elements for plate bending problems. For example, assemblages of the now well-known 12 degrees of freedom nonconforming rectangular model (Reference 9) always exhibit good convergence even though in some cases it is not monotonic. It is worth noting that there have been no reports of nonconvergence or of convergence to an incorrect answer with this element. For shell bending problems, this question is much more important, since a conforming element may require many more degrees of freedom than the nonconforming one. In some practical applications where the total number of degrees of freedom is limited by computer size, better results may sometimes be obtained with the nonconforming elements.

In the present work, an attempt is made to develop the simplest possible nonconforming representation for a cylindrical shell element. The radial or out-of-plane displacement component w is assumed to be a twelve-term polynomial in x and y, the longitudinal and circumferential coordinates of the element, respectively. This is the same displacement function used for the plate bending element discussed above. The in-plane displacement components u and v are each assumed in polynomial form up to linear terms in x and cubic terms in y. It will be seen subsequently that the higher order terms in y are required because of the shell curvature. The 28 arbitrary constants in these expressions for u, v and w are determined as functions of the seven generalized coordinates $\partial w / \partial x$, $\partial w / \partial y$, w, $\partial u / \partial y$, u, $\partial v / \partial y$ and v at each of the element corners. The expressions for u, v and w are then substituted into the strain energy and kinetic energy integrals from shell theory yielding 28 by 28 stiffness and mass matrices for the cylindrical shell element.

The rigid body modes incorporated in this element are determined by carrying out an eigenvalue analysis of these stiffness and mass matrices. It is found that all six rigid body degrees of freedom are adequately represented. The vibrations of a curved, cantilevered fan blade are then predicted with various element gridworks, and the results are verified experimentally.

SECTION II

THEORETICAL FORMULATION

DISPLACEMENTS

As pointed out on Page 22 of Reference 9, the first requirement of a finite element is that it must be capable of undergoing rigid body motions with little or no strain. Hence, the cylindrical shell element will require special displacement functions in order to ensure that all six rigid body modes are included. First, it is clear that the twelve term polynomial in x and y used for the plate bending element may be used here for the radial displacement w,

$$w(x,y) = a_1 + a_2 x + a_3 y + a_4 xy + a_5 x^2 + a_6 y^2 + a_7 x^2 y$$
$$+ a_8 xy^2 + a_9 x^3 + a_{10} y^3 + a_{11} x^3 y + a_{12} xy^3 \tag{1}$$

Second, since the element sides y = 0 and y = b (Figure 1) are straight, it will be sufficient to assume linear dependence on x for the in-plane displacements u and v. On the other hand, their dependence on y will have to be higher order than linear because of the shell curvature in that direction. This was shown clearly by early experience with a 20-degree of freedom model in which u and v were only linear in y. The complete results for this model which are given in the Appendixes of Reference 10 indicated that two of the required six rigid body modes were not adequately represented. Hence, cubic terms in y are included in the expressions for u and v as follows:

$$u(x,y) = a_{13} + a_{14} x + a_{15} y + a_{16} xy + a_{17} y^2$$
$$+ a_{18} xy^2 + a_{19} y^3 + a_{20} xy^3 \tag{2}$$

$$v(x,y) = a_{21} + a_{22} x + a_{23} y + a_{24} xy + a_{25} y^2$$
$$+ a_{26} xy^2 + a_{27} y^3 + a_{28} xy^3 \tag{3}$$

The 28 constants in Equations 1 to 3 are determined as functions of the 28 corner displacements w_{xi}, w_{yi} w_i, u_{yi}, u_i, v_{yi}, v_i, (i = 1,4) for the element ($w_x = \partial w / \partial x$, etc.). These are then substituted back into Equations 1 to 3, yielding expressions which completely define the displacements anywhere on the element in terms of the corner displacements.
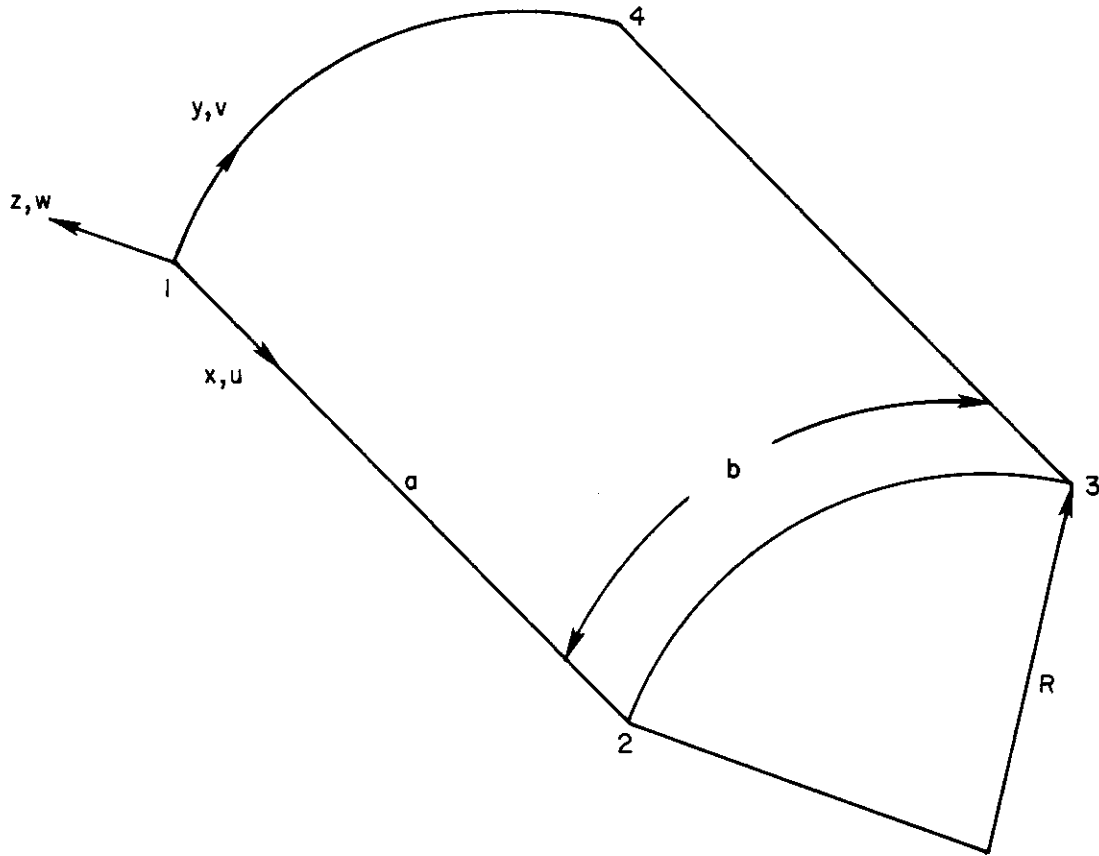
Figure 1. Cylindrical Shell Element

STRAIN ENERGY AND STIFFNESS MATRIX

The strain energy of an isotropic elastic, thin cylindrical shell element is given by (Reference 11)

$$U = \int_0^b \int_0^a \int_{-\frac{h}{2}}^{\frac{h}{2}} \frac{E}{2(1-\nu^2)} \left[\epsilon_x^2 + \epsilon_y^2 + 2\nu\epsilon_x\epsilon_y + \frac{1-\nu}{2}\epsilon_{xy}^2 \right] dz\,dx\,dy \qquad (4)$$

where E is Young's modulus and ν, Poisson's ratio. The strain displacement relations are

$$\epsilon_x = \frac{\partial u}{\partial x} - z\frac{\partial^2 w}{\partial x^2}$$

$$\epsilon_y = \frac{\partial v}{\partial y} + \frac{w}{R} - z\left(\frac{\partial^2 w}{\partial y^2} - \frac{1}{R}\frac{\partial v}{\partial y}\right) \qquad (5)$$

$$\epsilon_{xy} = \frac{\partial v}{\partial x} + \frac{\partial u}{\partial y} - 2z\left(\frac{\partial^2 w}{\partial x\,\partial y} - \frac{1}{R}\frac{\partial v}{\partial x}\right)$$

Substituting Equations 5 into Equation 4, and integrating through the shell thickness yields the strain energy expression, where $D = E\,h^3/12\,(1-\nu^2)$.

$$U = \frac{D}{2} \int_0^b \int_0^a \left\{ \left(\frac{\partial^2 w}{\partial x^2}\right)^2 + \left(\frac{\partial^2 w}{\partial y^2}\right)^2 + 2\nu \frac{\partial^2 w}{\partial x^2}\frac{\partial^2 w}{\partial y^2} + 2(1-\nu)\left(\frac{\partial^2 w}{\partial x \partial y}\right)^2 \right.$$

$$+ \frac{12}{h^2 R^2} w^2 + \frac{12}{h^2}\left[\left(\frac{\partial u}{\partial x}\right)^2 + \frac{1-\nu}{2}\left(\frac{\partial u}{\partial y}\right)^2\right] + \left(\frac{12}{h^2}+\frac{1}{R^2}\right)\left(\frac{\partial v}{\partial y}\right)^2$$

$$+ 2(1-\nu)\left(\frac{3}{h^2}+\frac{1}{R^2}\right)\left(\frac{\partial v}{\partial x}\right)^2 + \frac{24\nu}{h^2 R}w\frac{\partial u}{\partial x} + \frac{24}{h^2 R}w\frac{\partial v}{\partial y}$$

$$- \frac{2}{R}\frac{\partial^2 w}{\partial y^2}\frac{\partial v}{\partial y} - \frac{4(1-\nu)}{R}\frac{\partial^2 w}{\partial x \partial y}\frac{\partial v}{\partial x} - \frac{2\nu}{R}\frac{\partial^2 w}{\partial x^2}\frac{\partial v}{\partial y}$$

$$\left. + \frac{12}{h^2}\left[2\nu\frac{\partial u}{\partial x}\frac{\partial v}{\partial y} + (1-\nu)\frac{\partial u}{\partial y}\frac{\partial v}{\partial x}\right]\right\} dx\,dy \qquad (6)$$

The assumed displacement functions are substituted into Equation 6, and the integration over the midsurface of the shell element is carried out. The resulting strain energy expression is a quadratic function of the 28 corner displacements for the element, and may be written in the form

$$U = \frac{1}{2}\,\mathbf{W}^T\,\mathbf{K}\,\mathbf{W} \qquad (7)$$

where $\mathbf{W}$ is the nondimensional vector of nodal coordinates

$$\mathbf{W}^T = (w_{x1},\ w_{y1},\ w_1/a,\ u_{y1},\ u_1/a,\ v_{y1},\ v_1/a,\ w_{x2},\dots,$$

$$w_{x3},\dots,\ w_{x4},\dots \qquad (8)$$

and $\mathbf{K}$ is the element stiffness matrix given in Table I.

KINETIC ENERGY AND MASS MATRIX

The kinetic energy for the cylindrical element at any instant of time is (neglecting rotary inertia)

$$T = \frac{1}{2}\int_0^b \int_0^a \int_{-h/2}^{h/2} \rho\left[\left(\frac{\partial u}{\partial t}\right)^2 + \left(\frac{\partial v}{\partial t}\right)^2 + \left(\frac{\partial w}{\partial t}\right)^2\right] dz\,dx\,dy \qquad (9)$$

TABLE I

STIFFNESS MATRIX $\mathbf{K}/D$ FOR CYLINDRICAL SHELL ELEMENT*

SYMMETRICAL

$s = a/b, \quad q = a/R, \quad r = R/h,$

$p = r^2 q^4/2100, \quad \nu = \text{POISSON'S RATIO}$

The stiffness matrix is a symmetric lower-triangular array. The entries, read row by row, are:

```
k₁
k₂   k₃
k₄   k₅   k₆
k₇   k₈   k₉   k₁₀
k₁₁  k₁₂  k₁₃  k₁₄  k₁₅
k₁₆  k₁₇  k₁₈  0    k₁₉  k₂₀
k₂₁  k₂₂  k₂₃  -k₁₉ k₂₄  k₂₅  k₂₆
k₂₇  k₂₈  k₂₉  k₃₀  -k₁₁ k₃₁  k₃₂  k₁
-k₂₈ k₃₃  k₃₄  k₈   -k₁₂ k₃₅  k₃₆  -k₂   k₃
-k₂₉ k₃₄  k₃₇  k₉   -k₁₃ k₃₈  k₃₉  -k₄   k₅   k₆
-k₇  -k₈  -k₉  k₄₀  k₄₁  k₄₂  k₇   -k₈   -k₉  k₁₀
-k₁₁ -k₁₂ -k₁₃ k₄₁  k₄₃  k₄₄  k₁₁  -k₁₂  -k₁₃ k₁₄  k₁₅
-k₃₁ k₃₅  k₃₈  k₄₂  -k₄₄ k₄₅  k₄₆  k₁₆   -k₁₆ k₁₈  0    k₁₉  k₂₀
-k₃₂ k₃₆  k₃₉  -k₇  -k₄₂ k₄₇  -k₂₁ k₂₂   k₂₃  -k₁₉ k₂₄  k₂₅  k₂₆
```

(Lower rows of the triangular array, entries k_{48} through k_{82}, continue the symmetric block pattern for the remaining degrees of freedom; representative entries include $k_{48}, k_{49}, k_{50}, k_{51}, k_{52}, k_{53}, k_{54}, k_{55}, k_{56}, k_{57}, k_{58}, k_{59}, k_{60}, k_{61}, k_{62}, k_{63}, k_{64}, k_{65}, k_{66}, k_{67}, k_{68}, k_{69}, k_{70}, k_{71}, k_{72}, k_{73}, k_{74}, k_{75}, k_{76}, k_{77}, k_{78}, k_{79}, k_{80}, k_{81}, k_{82}$.)

TABLE I (cont.)

* WHERE

$$k_1 = \frac{4}{3s} + \frac{4(1-\nu)s}{15} + \frac{80p}{s^3} \; ; \; k_2 = \nu + \frac{63p}{s^2} \; ; \; k_3 = \frac{4s}{3} + \frac{4(1-\nu)s}{15} + \frac{80p}{s} \; ; \; k_4 = \frac{2}{s} + \frac{(1+4\nu)s}{5} + \frac{46p}{s} \; , \; k_5 = 2s^2 + \frac{1+4\nu}{5} + \frac{46p}{s^2}$$

$$k_6 = 4s^3 + \frac{4}{s} + \frac{2(7-2\nu)s}{5} + \frac{3454p}{s} \; ; \; k_7 = -\frac{\nu r^2 q^3}{20s} \; , \; k_8 = -\frac{2\nu r^2 q^3}{35s^2} \; , \; k_9 = -\frac{11\nu r^2 q^3}{35s} \; , \; k_{10} = \frac{r^2 q^2}{s}\left[\frac{4}{35s^2} + \frac{4(1-\nu)}{15}\right] \; , \; k_{11} = -\frac{7\nu r^2 q^3}{20s}$$

$$k_{12} = -\frac{11\nu r^2 q^3}{35s^2} \; ; \; k_{13} = -\frac{78\nu r^2 q^3}{35s} \; , \; k_{14} = r^2 q^2\left[\frac{22}{35s^2} + \frac{1-\nu}{5}\right] \; ; \; k_{15} = \frac{r^2 q^2}{s}\left[\frac{156}{35} + \frac{12(1-\nu)s^2}{5}\right] \; , \; k_{16} = \frac{q}{s}\left[\frac{r^2 q^2}{20} + \frac{\nu}{12}\right] \; ; \; k_{17} = \frac{q}{6}$$

$$k_{18} = \frac{q}{s}\left[\frac{5r^2 q^2}{12} + \frac{s^2}{3} + \frac{12-7\nu}{60}\right] \; ; \; k_{19} = \frac{3(1-3\nu)r^2 q^2}{10s} \; ; \; k_{20} = \frac{q^2}{s}\left[\frac{24r^2+2}{45} + \frac{(6r^2+2)(1-\nu)}{105s^2}\right] \; ; \; k_{21} = -q\left[\frac{3r^2 q^2}{10} + \frac{\nu}{2}\right] \; ; \; k_{22} = -\frac{q}{s}\left[\frac{2r^2 q^2}{5} + \frac{s^2}{3} + \frac{1-\nu}{5}\right]$$

$$k_{23} = q\left[-\frac{21r^2 q^2}{10} + \frac{2-3\nu}{2}\right] \; ; \; k_{24} = \frac{3(1+\nu)r^2 q^2}{2} \; ; \; k_{25} = q^2\left[\frac{12r^2+1}{30} + \frac{(33r^2+11)(1-\nu)}{105s^2}\right] \; ; \; k_{26} = \frac{q^2}{s}\left[\frac{(24r^2+2)s^2}{5} + \frac{(78r^2+26)(1-\nu)}{35}\right]$$

$$k_{27} = \frac{2}{35} - \frac{(1-\nu)s}{15} - \frac{60p}{s} \; ; \; k_{28} = -\frac{42p}{s^2} \; , \; k_{29} = \frac{2}{s} + \frac{(1-\nu)}{5} \; , \; k_{30} = \frac{\nu r^2 q^3}{20s} \; , \; k_{31} = -\frac{r^2 q^3}{30s} \; , \; k_{32} = \frac{r^2 q^3}{5} \; , \; k_{33} = \frac{q}{s}\left[\frac{11r^2 q^2}{60} + \frac{s^2}{6} - \frac{12-7\nu}{60}\right]$$

$$k_{34} = s^2 - \frac{1+4\nu}{5} + \frac{199p}{s^2} \; , \; k_{35} = \frac{q}{12} \; , \; k_{36} = \frac{q}{s}\left[-\frac{r^2 q^2}{5} - \frac{s^2}{6} + \frac{1-\nu}{5}\right] \; , \; k_{37} = 2s^3 - \frac{4}{s} - \frac{2(7-2\nu)s}{5} \; , \; k_{38} = \frac{q}{s}\left[\frac{11r^2 q^2}{60} + \frac{s^2}{6} - \frac{12-7\nu}{60}\right]$$

$$k_{39} = -q\left[\frac{9r^2 q^2}{10} + \frac{2-3\nu}{2}\right] \; , \; k_{40} = -\frac{r^2 q^2}{s}\left[-\frac{4}{35s^2} + \frac{2(1-\nu)}{15}\right] \; ; \; k_{41} = r^2 q^2\left[-\frac{22}{35s^2} + \frac{1-\nu}{10}\right] \; , \; k_{42} = -\frac{3(1+\nu)r^2 q^2}{10s} \; , \; k_{43} = \frac{r^2 q^2}{s}\left[-\frac{156}{35} + \frac{6(1-\nu)s^2}{5}\right]$$

$$k_{44} = \frac{3(1-3\nu)r^2 q^2}{2} \; , \; k_{45} = \frac{q^2}{s}\left[\frac{12r^2+1}{45} - \frac{(6r^2+2)(1-\nu)}{105s^2}\right] \; ; \; k_{46} = q^2\left[\frac{12r^2+1}{60} - \frac{(33r^2+11)(1-\nu)}{105s^2}\right] \; ; \; k_{47} = \frac{q^2}{s}\left[\frac{12r^2+1}{5} - \frac{(78r^2+26)(1-\nu)}{35}\right]$$

$$k_{48} = -\frac{1}{3s} + \frac{(1-\nu)s}{15} + \frac{30p}{s} \; , \; k_{49} = -\frac{28p}{s^2} \; ; \; k_{50} = \frac{1}{s} - \frac{(1-\nu)}{5} \; ; \; k_{51} = \frac{116p}{s} \; , \; k_{52} = \frac{3\nu r^2 q^3}{20s} \; , \; k_{53} = \frac{2}{3s} - \frac{4(1-\nu)s}{15} + \frac{40p}{s}$$

$$k_{54} = -\frac{1}{s} + \frac{(1+4\nu)s}{5} + \frac{199p}{s} \; , \; k_{55} = \frac{s}{3} + \frac{1-\nu}{15} \; , \; k_{56} = s^2 - \frac{1-\nu}{5} - \frac{30p}{s^3} \; , \; k_{57} = \frac{3\nu r^2 q^3}{70s^2} \; , \; k_{58} = \frac{13\nu r^2 q^3}{70s^2} \; , \; k_{59} = q\left[\frac{r^2 q^2}{30s^2} + \frac{1}{12} - \frac{1-\nu}{30s^2}\right]$$

$$k_{60} = \frac{2s}{3} - \frac{1-\nu}{15s} - \frac{60p}{s^3} \; ; \; k_{61} = 2s^2 + \frac{1-\nu}{5} - \frac{274p}{s^2} \; , \; k_{62} = q\left[\frac{r^2 q^2}{15s^2} + \frac{1}{6} + \frac{1-\nu}{30s^2}\right] \; , \; k_{63} = -2s^3 - \frac{2}{s} + \frac{2(7-2\nu)s}{5} + \frac{394p}{s} \; , \; k_{64} = -\frac{13\nu r^2 q^3}{70s}$$

$$k_{65} = -\frac{27\nu r^2 q^3}{35s} \; , \; k_{66} = q\left[-\frac{9r^2 q^2}{10} + \frac{2-\nu}{2}\right] \; ; \; k_{67} = -4s^3 - \frac{4}{s} + \frac{2(7-2\nu)s}{5} + \frac{1226p}{s} \; , \; k_{68} = -q\left[\frac{21r^2 q^2}{10} + \frac{2-\nu}{2}\right] \; ; \; k_{69} = \frac{r^2 q^2}{s}\left[\frac{3}{35s^2} - \frac{1-\nu}{30}\right]$$

$$k_{70} = r^2 q^2\left[\frac{13}{35s^2} + \frac{1-\nu}{10}\right] \; , \; k_{71} = \frac{(1+\nu)r^2 q^2}{20s^2} \; , \; k_{72} = -\frac{r^2 q^2}{s}\left[\frac{3}{35s^2} + \frac{1-\nu}{15}\right] \; ; \; k_{73} = r^2 q^2\left[-\frac{13}{35s^2} + \frac{1-\nu}{5}\right] \; , \; k_{74} = -\frac{(1-3\nu)r^2 q^2}{20s^2}$$

$$k_{75} = -\frac{r^2 q^2}{s}\left[\frac{54}{35} + \frac{6(1-\nu)s^2}{5}\right] \; , \; k_{76} = \frac{r^2 q^2}{s}\left[\frac{54}{35} - \frac{12(1-\nu)s^2}{5}\right] \; , \; k_{77} = -\frac{q^2}{s}\left[-\frac{12r^2+1}{180} + \frac{(3r^2+1)(1-\nu)}{70s^2}\right] \; , \; k_{78} = q^2\left[\frac{12r^2+1}{60} + \frac{(39r^2+13)(1-\nu)}{210s^2}\right]$$

$$k_{79} = -\frac{q^2}{s}\left[\frac{12r^2+1}{90} + \frac{(3r^2+1)(1-\nu)}{70s^2}\right] \; ; \; k_{80} = q^2\left[\frac{12r^2+1}{30} + \frac{(39r^2+13)(1-\nu)}{210s^2}\right] \; ; \; k_{81} = \frac{q^2}{s}\left[\frac{12r^2+1}{5} + \frac{(27r^2+9)(1-\nu)}{35}\right] \; ; \; k_{82} = \frac{q^2}{s}\left[-\frac{24r^2+2}{5} + \frac{(27r^2+9)(1-\nu)}{35}\right]$$

where ρ is the shell material density. Assuming that the displacements are sinusoidal in time, and integrating through the shell thickness yields

$$T = \frac{\omega^2}{2} \int_0^b \int_0^a \rho h \left[u^2 + v^2 + w^2 \right] dx\, dy \qquad (10)$$

where ω is the frequency of motion.

The assumed displacements are substituted into Equation 10, and the integration over the midsurface of the element is carried out. This yields the quadratic form

$$T = \frac{\omega^2}{2} \mathbf{W}^T \mathbf{M} \mathbf{W} \qquad (11)$$

where $\mathbf{M}$ is the element mass matrix given in Table II.

TABLE II

MASS MATRIX **M** × 25200s³/ρha⁴ FOR CYLINDRICAL SHELL ELEMENT

SYMMETRICAL

$s = \dfrac{a}{b}$

1	2	3	4	5	6	7	8	9	10	11	12	13	14	15	16	17	18	19	20	21	22	23	24	25	26	27	28
$80s^2$																											
$63s$	80																										
$461s^2$	$461s$	$3454s^2$																									
0	0	0	80																								
0	0	0	$440s$	$3120s^2$																							
0	0	0	0	0	80																						
0	0	0	0	0	$440s$	$3120s^2$																					
$-60s^2$	$-42s$	$-274s^2$	0	0	0	0	$80s^2$																				
$42s$	40	$199s$	0	0	0	0	$-63s$	80																			
$274s^2$	$199s$	$1226s^2$	0	0	0	0	$-461s^2$	$-461s$	$3454s^2$																		
0	0	0	40	$220s$	0	0	0	0	0	80																	
0	0	0	$220s$	$1560s^2$	0	0	0	0	0	$440s$	$3120s^2$																
0	0	0	0	0	-30	$-130s$	0	0	0	0	0	80															
0	0	0	0	0	$130s$	$540s^2$	0	0	0	0	0	$440s$	$3120s^2$														
$-30s^2$	$-28s$	$-116s^2$	0	0	0	0	$40s^2$	$42s$	$-199s^2$	0	0	0	0	$80s^2$													
$-28s$	-30	$-116s$	0	0	0	0	$42s$	-60	$-274s$	0	0	0	0	$63s$	80												
$116s^2$	$116s$	$394s^2$	0	0	0	0	$-199s^2$	$-274s$	$1226s^2$	0	0	0	0	$-461s^2$	$-461s$	$3454s^2$											
0	0	0	-30	$-130s$	0	0	0	0	0	-60	$-260s$	0	0	0	0	0	80										
0	0	0	$130s$	$540s^2$	0	0	0	0	0	$260s$	$1080s^2$	0	0	0	0	0	$440s$	$3120s^2$									
0	0	0	0	0	-60	$-260s$	0	0	0	0	0	-30	$-130s$	0	0	0	0	0	80								
0	0	0	0	0	$260s$	$1080s^2$	0	0	0	0	0	$130s$	$540s^2$	0	0	0	0	0	$440s$	$3120s^2$							
$40s^2$	$42s$	$199s^2$	0	0	0	0	$-30s^2$	$28s$	$-116s^2$	0	0	0	0	$-60s^2$	$42s$	$274s^2$	0	0	0	0	$80s^2$						
$-42s$	-60	$-274s$	0	0	0	0	$28s$	-30	$116s$	0	0	0	0	$42s$	40	$-199s$	0	0	0	0	$-63s$	80					
$199s^2$	$-274s$	$1226s^2$	0	0	0	0	$-116s^2$	$116s$	$394s^2$	0	0	0	0	$274s^2$	$-199s$	$1226s^2$	0	0	0	0	$461s^2$	$-461s$	$3454s^2$				
0	0	0	-60	$-260s$	0	0	0	0	0	-30	$-130s$	0	0	0	0	0	40	$-220s$	0	0	0	0	0	80			
0	0	0	$260s$	$1080s^2$	0	0	0	0	0	$130s$	$540s^2$	0	0	0	0	0	$-220s$	$1560s^2$	0	0	0	0	0	$-440s$	$3120s^2$		
0	0	0	0	0	-60	$-260s$	0	0	0	0	0	40	$-220s$	0	0	0	0	0	-30	$-130s$	0	0	0	0	0	80	
0	0	0	0	0	$260s$	$1080s^2$	0	0	0	0	0	$-220s$	$1560s^2$	0	0	0	0	0	$130s$	$540s^2$	0	0	0	0	0	$-440s$	$3120s^2$

SECTION III

RIGID BODY MODES

A simple check of this finite element model can be made by using it to determine the free-free vibrations of a rectangular section of a cylindrical shell. The six lowest modes for this problem are rigid body modes with zero frequency, and an approximate solution using one finite element should include these modes.

Thus, the first test for the present model is to determine the eigenvalues and eigenvectors for the matrix equation

$$\left[K - \lambda M \right] W = 0 \tag{12}$$

where K and M are the 28 by 28 stiffness and mass matrices given in Tables I and II, respectively, W is the displacement vector given by Equation 8, and $\lambda = \rho \, hab^3 \omega^2 / 25200 \, D$ is the nondimensional eigenvalue. Carrying this out for $\nu = 0.3$, r = 200.0, s = 1.0, and q = 0.5 (see Table I for definitions) yields the seven lowest eigenvalues: 0.4813×10^{-14}, 0.8912×10^{-14}, 0.2108×10^{-9}, 0.2379×10^{-7}, 0.1920×10^{-5}, 0.1951×10^{-5} and 0.7887×10^{-2}.

The first two eigenvalues are essentially zero to the accuracy of the double precision calculations. The two associated eigenvectors represented combinations of rigid body motion of the shell element in the longitudinal and circumferential directions. It was found that suitable linear combinations of these two eigenvectors would yield pure rigid body motion in either the longitudinal or circumferential directions alone. Hence, the first two rigid body modes predicted by the cylindrical shell element were pure "translations" in u and v.

The next four eigenvalues, while not exactly zero, are quite small relative to the seventh one. This last eigenvalue corresponds to the first true vibration mode for the free-free shell segment and is within a few percent of the corresponding flat plate solution (Reference 10). The eigenvectors associated with eigenvalues three to six were very good approximations of the following rigid body motions: number three was a translation parallel to a normal at x = a/2 and y = b/2, number four was a rotation about the same normal, number five was a rotation about a cylindrical generator through y = b/2, and finally, number six was a rotation about a chord at x = a/2.

Hence, it may be concluded that the cylindrical shell element provides an adequate representation of all six rigid body modes.

SECTION IV

VIBRATIONS OF CANTILEVERED CURVED PLATES

A problem of considerable practical importance that is not amenable to ordinary analytical methods is that of the vibration of curved fan blades. Such a fan blade is depicted in Figure 2. This blade is a rectangular section of a cylindrical shell where y = 0, and y = W are parallel cylinder generators. The curved edge x = L is considered built-in or clamped to an infinitely rigid foundation, while the other three sides are free. The thickness is h, and the radius of curvature is R.

EXPERIMENT

An experimental model of the fan blade shown in Figure 2 was constructed by rolling a piece of sheet steel 0.120 inches thick to a radius of curvature of 24.0 inches. This curved sheet was then cut to size (W = L = 12.0 inches) and welded to a 4.0 x 4.0 x 16.0 inches steel block to simulate the clamped boundary condition indicated in Figure 2. The vibration modes of this blade were excited by a sinusoidal magnetic force, and the mode shapes were determined by sand pattern observations and measurements with an inductance pick-up.
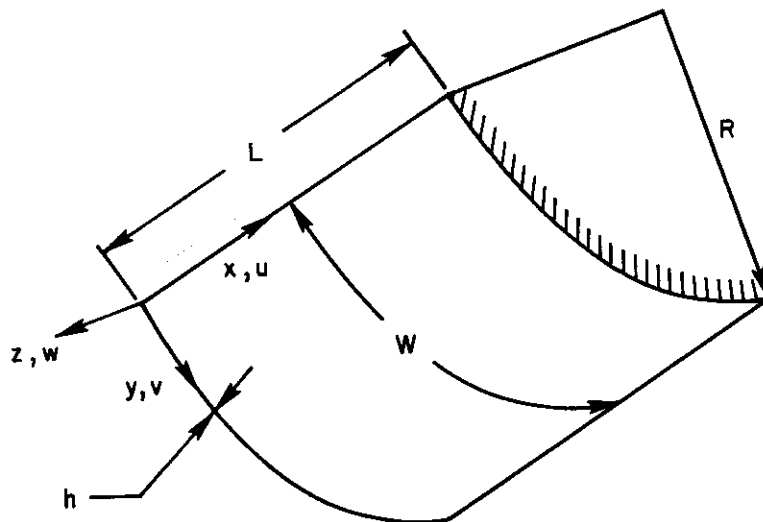
Figure 2. Curved Fan Blade

The first twelve vibration frequencies for this fan blade are given in Table III along with sketches of the corresponding nodal patterns. See Figure 3 for more detailed drawings of the experimental nodal patterns and tip deflections. The experimental results presented in Table III are reasonably clear and need little discussion here. It is interesting to note that the first "torsion" mode, one, occurs at a lower frequency than the first "bending" mode, two. This is the reverse of what would occur if the blade were flat and is a result of the stiffening due to the blade curvature.

Some of the experimental nodal patterns and tip deflections presented in Figure 3 exhibit a noticeable amount of asymmetry with respect to the center line of the blade. This asymmetry must be associated with residual stresses induced by the rolling and welding processes.
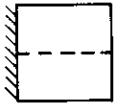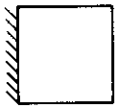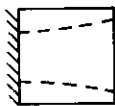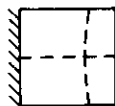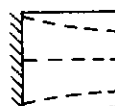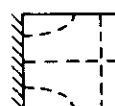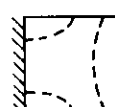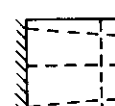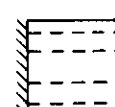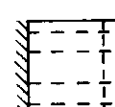
THEORY

Theoretical predictions of the vibration modes for the fan blade described above were calculated with various combinations of the shell elements developed herein. The process for setting up the eigenvalue problem for a given assemblage of finite elements is fairly standard now, and need only be described briefly here. At each element corner junction, all the generalized coordinates are made continuous and the sums of the corresponding forces (ordinary plus D'Alembert's) are set equal to zero. All the generalized coordinates vanish at the clamped edge, $x = L$ in Figure 2. Square elements (i.e. $s = 1.0$) were used in all the calculations.

The computations were carried out for various assemblages of elements up to a 4 x 4 grid representation. However, before discussing the results in detail, it must be pointed out that the approximation of neglecting in-plane inertia was used in evaluating the 3 x 3 and 4 x 4 grid results. This approximation was required in order to reduce the order of the eigenvalue problems to a practical size. It is worth noting that the neglecting of in-plane inertia is fairly standard procedure in most shell dynamic problems and was carried out by straightforward matrix partitioning. The reader is referred to Reference 10 for complete details. The validity of this approximation was verified (Reference 10) by carrying out the calculations for a 2 x 2 grid representation of the fan blade with and without the inclusion of in-plane inertia.

The complete results shown in Table III merit detailed study especially as to how the predicted frequencies change with refinement of the finite element assemblages. It may be noted that in general these frequencies converge very rapidly towards the experimental values. Furthermore, the convergence appears to be monotonic. The only possible exceptions may be modes three and twelve where the predicted frequencies appear to undershoot the experimental values slightly. However, the differences are well within the possible experimental error.

259

TABLE III VIBRATION FREQUENCIES FOR CURVED FAN BLADE

APPROXIMATE MODE SHAPE		EXPERIMENT	FINITE ELEMENT GRIDS			
			1 x 1	2 x 2	3 x 3	4 x 4
		(cps)	(cps)	(cps)	(cps)	(cps)
1		86·6	189·10	122·24	100·71	93·47
2		135·5	266·25	179·67	155·09	147·64
3		258·9	431·01	278·71	260·94	255·14
4		350·6		485·04	430·03	393·08
5		395·2		495·80	452·90	423·50
6		531·1		608·05	535·03	534·30
7		743·2			798·30	781·51
8		751·2			820·41	792·16
9		792·1			891·29	863·20
10		809·2			891·16	862·35
11		996·8			1121·25	1001·56
12		1215·0				1175·37

Finally, it may be noted from Table III that the first 12 vibration frequencies for the curved fan blade are predicted to within 10 percent by the 4 x 4 grid of finite elements.

The fact that the convergence is apparently monotonic although highly gratifying is rather surprising, in light of the experiences with flat plate elements. In particular, it has been found that the nonconforming plate elements exhibit some nonmonotonic convergence when used to solve the comparable cantilevered flat plate problem. For example, as shown in Table II(c) of Reference 12, the predicted frequencies for modes four and five are overpredicted with one element and then underpredicted with a 2 x 2 grid of elements. It must be emphasized, however, that the present results are true only for the particular shell configuration considered herein, and it is not clear how they would change with changes in radius-to-thickness or radius-to-width ratios.

The fan blade vibration nodal patterns and tip deflections as obtained from the 4 x 4 grid of finite elements are given by the solid curves in Figure 3. These may be compared to the experimental results obtained from sand patterns and inductance pick-up measurements and shown as dashed curves in these figures. For most of the modes, the agreement between experiment and theory is extremely good. This is especially true for modes one to six inclusive. The most notable discrepancies occur for modes seven and ten. It is interesting to note, on the other hand, that modes 8 and 9 which are the "symmetric twins" for modes seven and ten, respectively, are predicted much better by the theory. It is not clear why this should be so, but it does suggest that the present cylindrical shell element is more capable of predicting symmetric modes which require less twisting than the antisymmetric ones. Finally, the agreement between theory and experiment for the higher modes 11 and 12 again becomes quite good.

At this point, it is worth considering the effect of curvature on the fan blade vibrations in more detail. Calculations were carried out for various values of radius-to-thickness ratio R/h up to 200.0 using the 4 x 4 grid of finite elements, and the results are shown in Figure 4. Note that the length-to-thickness ratio L/h was held constant at 100.0 for these calculations. The lowest two modes are not shown in the figure because their nodal line patterns did not change, but the numerical results for the frequency squared parameter $\rho h \omega^2 L^4 / D$ did change as follows:

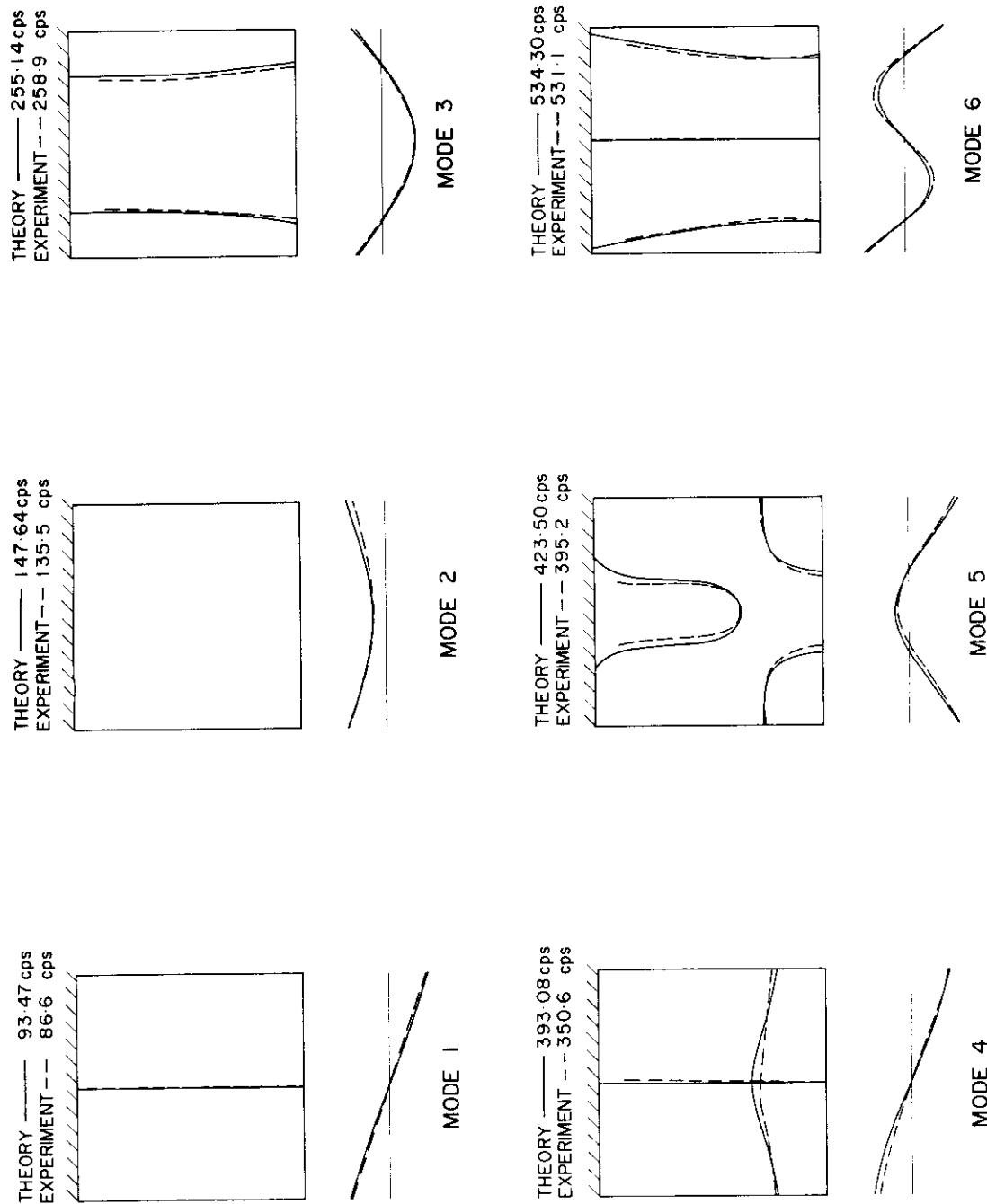| R/h	∞	1000	500	300	200
Mode 1	12.0367	29.543	78.978	182.784	331.536
Mode 2	72.597	75.400	83.391	100.927	132.889

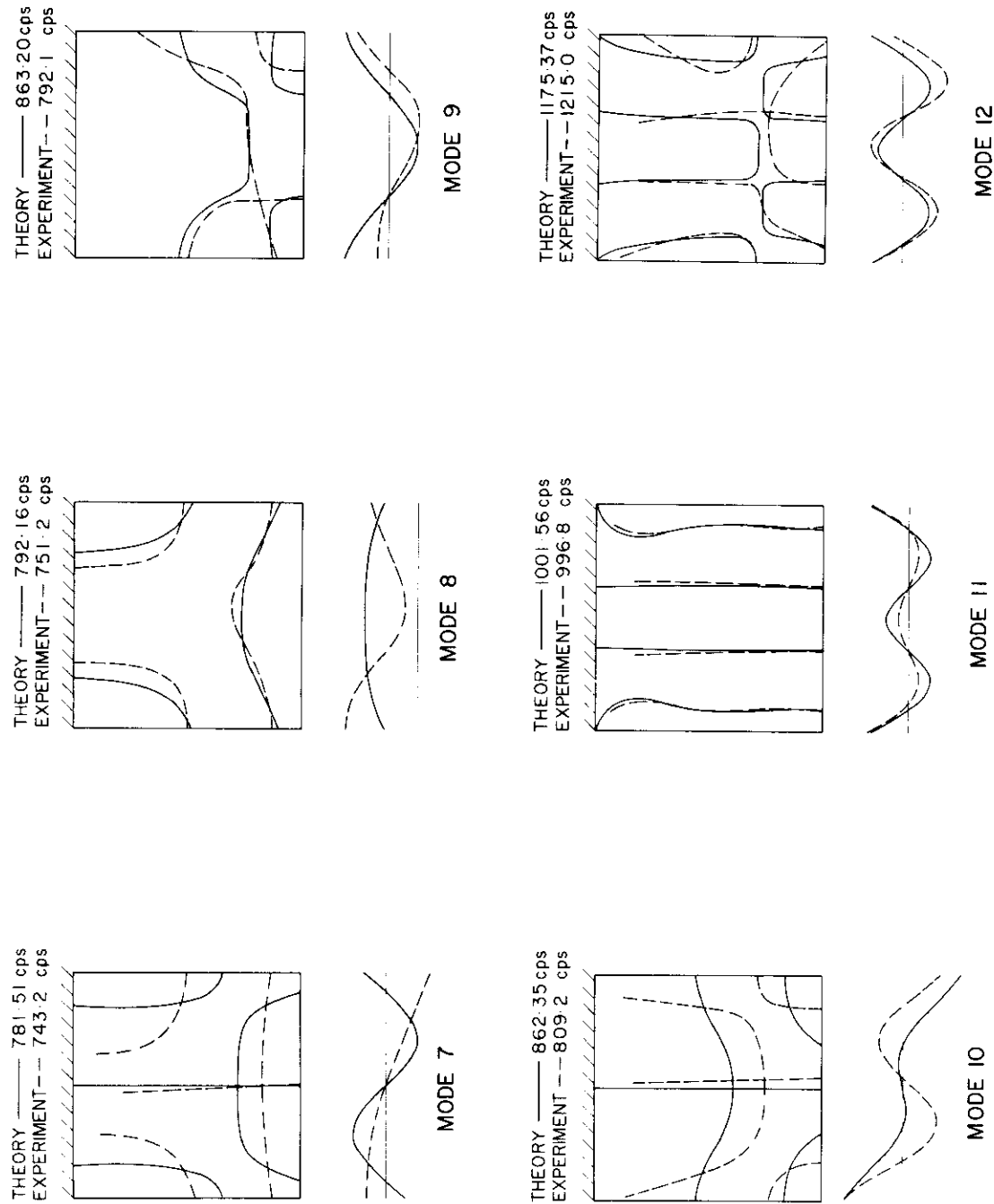Figure 3. Comparison of Theoretical and Experimental Mode Shapes

Figure 3. Comparison of Theoretical and Experimental Mode Shapes

The numerical results given above and in Figure 4 for the flat plate case (R/h = ∞) were obtained in Reference 13 using a 4 x 4 grid of finite plate elements. These results were compared to "exact series solutions" in Reference 13, and it was found that the first nine frequencies (not frequencies squared) were correct to within about 2.5 percent.

The results shown in Figure 4 exhibit some quite surprising effects. One would expect the curvature to have only a small effect on modes predominated by nodal lines normal to the clamped boundary. This idea is partially verified for modes two, eight, and sixteen and to a lesser extent by modes 10 and 15, but it is completely refuted by the results for modes four, six and thirteen, since their nodal patterns are fundamentally changed by the increasing curvature. On the other hand, as one would expect, the effect of curvature on modes with nodal lines parallel to the clamped boundary is very pronounced. This is especially evident for mode one, (the clamped boundary is considered to be a nodal line here) where the frequency squared parameter has increased by a factor of 25. Other examples showing significant changes are modes three, seven, nine, and twelve. It is especially interesting to note the apparent interchange of nodal line patterns between modes three and four, and twelve and thirteen with increasing curvature.
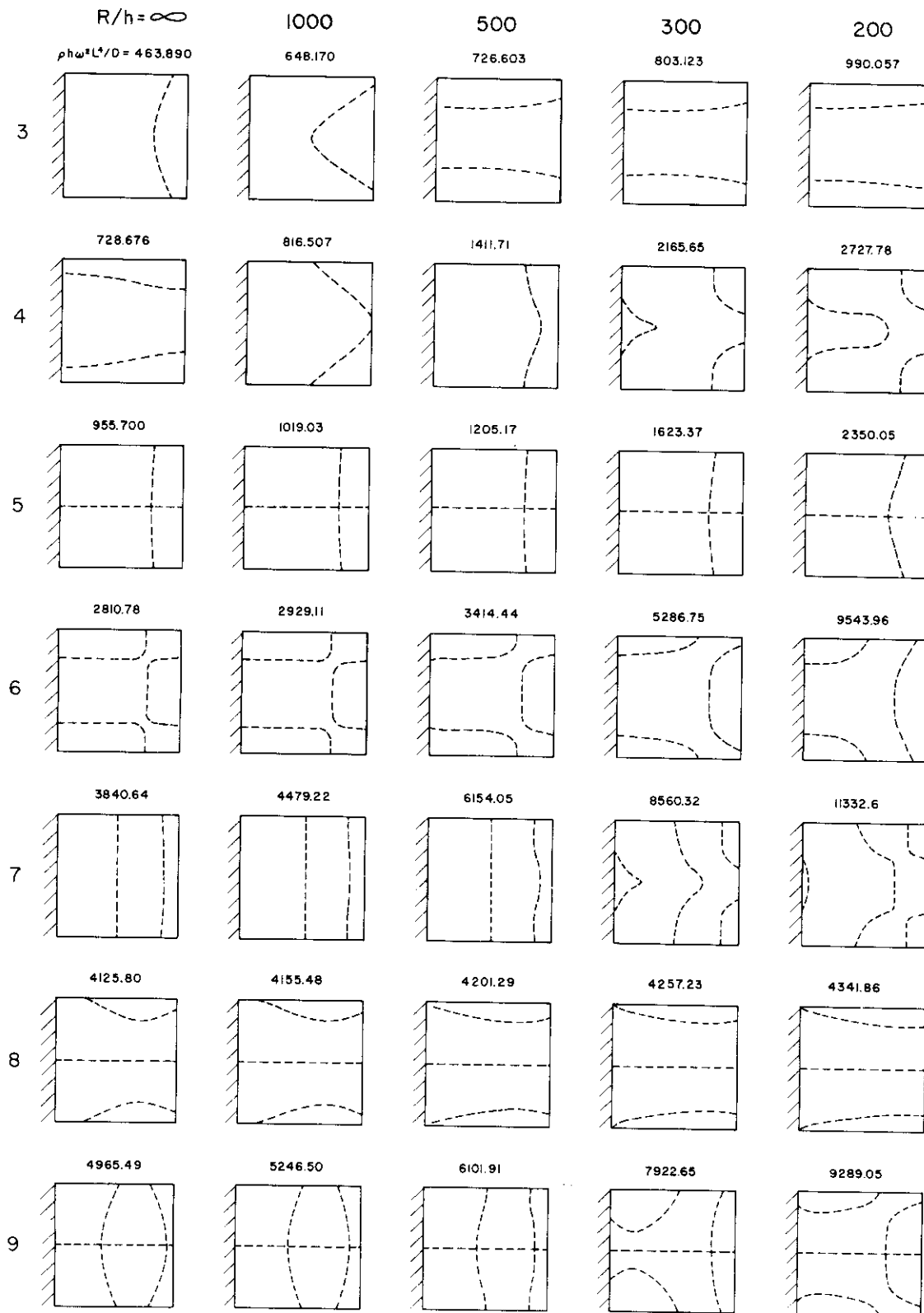
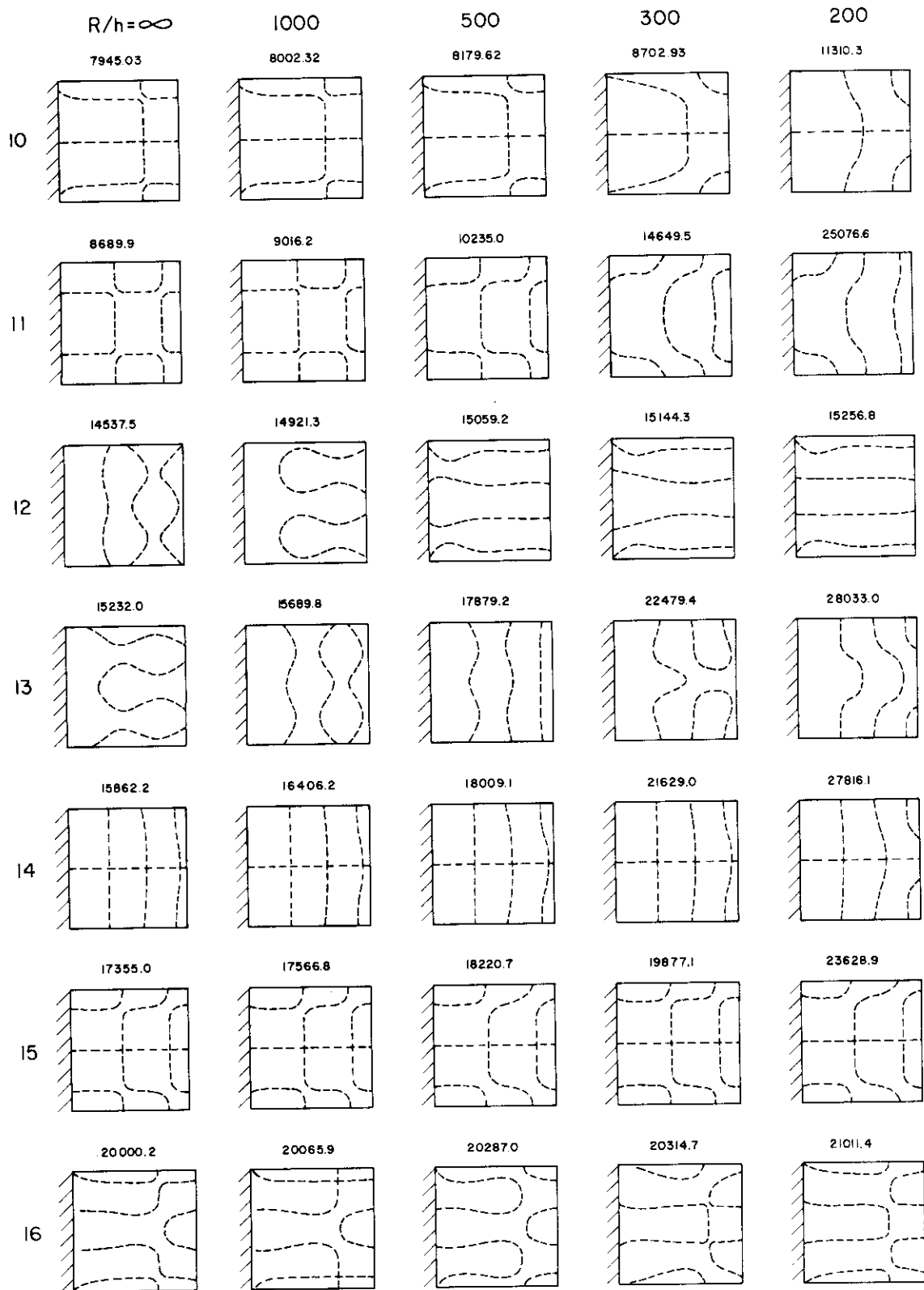Figure 4.   Effect of Curvature on Fan Blade Vibrations

Figure 4. Effect of Curvature on Fan Blade Vibrations

SECTION V

CONCLUDING REMARKS

The stiffness and mass matrices for a relatively simple finite cylindrical shell element have been presented. This element has 28 degrees of freedom corresponding to the seven generalized coordinates $\partial w/\partial x$, $\partial w/\partial y$, w, $\partial u/\partial y$, u, $\partial v/\partial y$ and v at each corner. It was found from an eigenvalue analysis of the stiffness and mass matrices that all six rigid body modes were adequately represented.

The element was used to predict vibration modes and frequencies for a curved, cantilevered fan blade, and the results were verified experimentally. It was found that a 4 x 4 grid of the finite elements predicted the first twelve vibration frequencies to within ten percent. The agreement between the experimental and theoretical mode shapes was generally very good. These finite elements should prove extremely useful for static or dynamic problems involving rectangular portions of cylindrical shells, especially since such configurations are very difficult to analyze by ordinary analytical techniques.

SECTION VI

REFERENCES

1. Jones, R. E. and Strome, D. R., "A Survey of Analysis of Shells by the Displacement Method." In Matrix Methods in Structural Mechanics, Wright-Patterson AFB, AFFDL-TR-66-80, 1966.

2. Hrennikoff, A. and Tezcan, S. S., "Analysis of Cylindrical Shells by the Finite Element Method." Symposium on Problems of Interdependence of Design and Construction of Large-Span Shells for Industrial and Civic Buildings," Leningrad, U. S.S.R., September 6-9, 1966.

3. Clough, R. W. and Johnson, C. P., "A Finite Element Approximation for the Analysis of Thin Shells." Int. J. of Solids and Structures, Vol. 4, pp. 43-60, 1968.

4. Utku, S. and Melosh, R. J., "Behavior of Triangular Shell Element Stiffness Matrices Associated with Polyhedral Deflection Distributions." AIAA Paper no. 67-114, AIAA Sixth Aerospace Sciences Meeting, New York, January 23-26, 1967. (Also AIAA J., Vol. 6, pp. 374-376, 1968).

5. Bogner, F. K., Fox, R. L. and Schmit, L. A., "A Cylindrical Shell Discrete Element." AIAA J., Vol. 5, pp. 745-750, 1967.

6. Timoshenko, S. and Woinowsky-Krieger, S., "Theory of Plates and Shells." McGraw-Hill Book Co., Inc., New York, pp. 501-506, 1959.

7. Tong, P. and Pian, T.H.H., "The Convergence of Finite Element Method in Solving Linear Elastic Problems." Int. J. of Solids and Structures, Vol. 3, pp. 865-879, 1967.

8. Cantin, G. and Clough, R. W., "A Curved, Cylindrical-Shell, Finite Element." AIAA J., Vol. 6, pp. 1057-1062, 1968.

9. Zienkiewicz, O. C., The Finite Element Method in Structural and Continuum Mechanics. McGraw-Hill Publishing Co. Ltd., London, 1967.

10. Olson, M. D. and Lindberg, G. M., <u>A Finite Cylindrical Shell Element and the Vibrations of a Curved Fan Blade.</u> National Research Council of Canada Aeronautical Report LR-497, February, 1968.

11. Love, A. E. H., "Mathematical Theory of Elasticity." Cambridge University Press, 4th Ed., pp. 529 and 543, 1927.

12. Dawe, D. J., "A Finite Element Approach to Plate Vibration Problems." J. of Mech. Eng. Science, Vol. 7, pp. 28-32, 1965.

13. Lindberg, G. M. <u>The Vibration of Stepped Cantilevered Plates.</u> National Research Council of Canada Aeronautical Report LR-494, December, 1967.